the plant journal

SEB Society for Experimental Biology

The Plant Journal (2013) doi: 10.1111/tpj.12214

Targeted transcriptomic and metabolic profiling reveals temporal bottlenecks in the maize carotenoid pathway that may be addressed by multigene engineering

Gemma Farré[1,†], Sol Maiam Rivera[2,†], Rui Alves[3], Ester Vilaprinyo[3], Albert Sorribas[3], Ramon Canela[2], Shaista Naqvi[1,‡], Gerhard Sandmann[4], Teresa Capell[1], Changfu Zhu[1] and Paul Christou[1,5,*]

[1]*Department of Plant Production and Forestry Science, School of Agrifood and Forestry Science and Engineering (ETSEA), University of Lleida/Agrotecnio Center, Avenida Alcalde Rovira Roure 191, 25198 Lleida, Spain,*

[2]*Department of Chemistry, School of Agrifood and Forestry Science and Engineering (ETSEA), University of Lleida/Agrotecnio Center, Avenida Alcalde Rovira Roure 191, 25198 Lleida, Spain,*

[3]*Department Ciències Mèdiques Bàsiques, University of Lleida & Institut de Recerca Biomèdica de Lleida, Edifici Recerca Biomèdica I, Avenida Alcalde Rovira Roure 80, 25198 Lleida, Spain,*

[4]*Biosynthesis Group, Molecular Biosciences, Johann Wolfgang Goethe Universität, D–60054 Frankfurt, Germany, and*

[5]*Institució Catalana de Recerca I Estudis Avançats, 08010 Barcelona, Spain*

Received 13 February 2013; revised 02 April 2013; accepted 12 April 2013.

*For correspondence (e-mail christou@pvcf.udl.es).

†These authors contributed equally to this work.

‡Present address: Division MRC Protein Phosphorylation Unit, Sir James Black Complex, University of Dundee, Dundee, DD1 5EH, UK.

SUMMARY

Carotenoids are a diverse group of tetraterpenoid pigments found in plants, fungi, bacteria and some animals. They play vital roles in plants and provide important health benefits to mammals, including humans. We previously reported the creation of a diverse population of transgenic maize plants expressing various carotenogenic gene combinations and exhibiting distinct metabolic phenotypes. Here we performed an in-depth targeted mRNA and metabolomic analysis of the pathway to characterize the specific impact of five carotenogenic transgenes and their interactions with 12 endogenous genes in four transgenic lines representing distinct genotypes and phenotypes. We reconstructed the temporal profile of the carotenoid pathway during endosperm development at the mRNA and metabolic levels (for total and individual carotenoids), and investigated the impact of transgene expression on the endogenous pathway. These studies enabled us to investigate the extent of any interactions between the introduced transgenic and native partial carotenoid pathways during maize endosperm development. Importantly, we developed a theoretical model that explains these interactions, and our results suggest genetic intervention points that may allow the maize endosperm carotenoid pathway to be engineered in a more effective and predictable manner.

Keywords: metabolic engineering, *Zea mays*, carotenoids, ketocarotenoids, transcriptomic analysis, metabolic profiling, endosperm development.

INTRODUCTION

Carotenoids are a group of approximately 800 lipid-soluble organic molecules whose spectral properties are responsible for the yellow, orange and red colors of the tissues in which they accumulate (Britton *et al.*, 2004). Carotenoids are synthesized by all photosynthetic organisms and many non-photosynthetic bacteria, as well as certain fungi and animals (Moran and Jarvik, 2010). In plants, carotenoids fulfil two essential functions during photosynthesis: light harvesting and protection of the photosynthetic apparatus from photo-oxidation (Demmig-Adams and Adams, 1996). In plants, the synthesis of carotenoids is initiated by the enzyme phytoene synthase (PSY), which condenses two molecules of genarylgeranyl diphosphate to form 15–*cis*-phytoene (Misawa *et al.*, 1994). Four desaturation steps catalyzed by phytoene desaturase (PDS), ζ –carotene isomerase (Z–ISO) and ζ–carotene desaturase (ZDS) produce the first colored carotene (pro-lycopene). This is converted to all-*trans*-lycopene by carotene isomerase (CRTISO) in non-green tissues and by light in green tissues (Chen *et al.*, 2010; Li *et al.*, 2010). In bacteria, a single enzyme

encoded by the *crt*I gene accomplishes all the desaturation and isomerization steps and produces all-*trans*-lycopene from 15–*cis*-phytoene directly (Bai *et al.*, 2011; Figure 1).

Lycopene is an important branch point in the carotenoid pathway because it serves as the substrate for two competing enzymes that cyclize the free ends, lycopene β–cyclase (LYCB) and lycopene ε–cyclase (LYCE; Bai *et al.*, 2011). In the α branch, the addition of one ε–ring and one β–ring generates α–carotene, which is converted into zeinoxanthin by the di-iron non-heme β–carotene hydroxylase (BCH) and/or the P450-type β–carotene hydroxylases CYP97A and CYP97B, and then into the yellow pigment lutein by the P450-type β–hydroxylase CYP97C (Bai *et al.*, 2011). In the β branch, the addition of two β–rings generates β–carotene, which is converted into β–cryptoxanthin and then zeaxanthin by BCH and/or CYP97A and/or CYP97B (Quinlan *et al.*, 2007; Kim *et al.*, 2010).

In both prokaryotes and eukaryotes, β–carotene may be converted into astaxanthin in alternative reactions catalyzed by β–carotene ketolase and β–carotene hydroxylase (HYDB), which may involve BCH, CYP97A or CYP97B catalyzing the same enzymatic step in the pathway (Figure 1).

Phytoene synthase (PSY), the first committed step in the carotenoid pathway, is the major rate-limiting step in the endosperm of maize (*Zea mays*) (Zhu *et al.*, 2008). Endosperm-specific expression of *psy1* in white maize relieves this bottleneck, increasing the total carotene content and leading to predominant accumulation of lutein and zeaxanthin (Zhu *et al.*, 2008). The LYCE/LYCB ratio is a flux control point and determines the β:α branch carotenoid ratio (Farré *et al.*, 2011). Over-expressing LYCB shifts the balance towards the β branch, enhancing β–carotenoids at the expense of α–carotene and lutein, whereas over-expressing LYCE has the opposite effect (e.g. Rosati *et al.*, 2000; D'Ambrosio *et al.*, 2004). Transgenic canola (*Brassica napus*) seeds expressing *crt*B (PSY), *crt*I and *crt*Y (LYCB) contained more carotenoids than wild-type seeds (Ravanello *et al.*, 2003). In transgenic maize endosperm expressing *psy1*, *crt*I and *lycb*, the β:α ratio increased from 1.2 to 3.5 (Zhu *et al.*, 2008). Nevertheless, there was also enhanced flux through the α–branch of the pathway, producing almost 25 times more lutein than normal (up to 13.12 μg g^{-1} dry weight). These examples show that the relationship between gene expression levels in the carotenoid biosynthesis pathway and the control of the flux through each branch of the pathway is difficult to predict. Even when the metabolic flux is shifted towards β–carotene, there is still enough flux through the alternative branch of the pathway to produce more than enough lutein (Naqvi *et al.*, 2011).

Another important reaction in the carotenoid pathway is the conversion of β–carotene to zeaxanthin by BCH. Silencing the *bch* gene in potato tubers (*Solanum tuberosum*) enhanced β–carotene and lutein levels at the expense of zeaxanthin (Van Eck *et al.*, 2007). The carotenoid content of crops may be reduced substantially by the further conversion of zeaxanthin to violaxanthin, representing another potential intervention target because epoxy carotenoids (violaxanthin and neoxanthin) are precursors of abscisic acid. Activating absicisic acid production could then deplete the carotenoid content. In order to gain insight into the relationship between the expression of carotenogenic genes, the production and accumulation of various carotenoids, and flux through various steps and branches that are bottlenecks in wild-type plants, we selected representative transgenic lines for in-depth mRNA and carotenoid profiling. This was performed in order to investigate the effects of specific interactions between five carotenogenic transgenes and 12 endogenous genes on the flux through each step and branching point of the carotenoid pathway. To do so we created four transgenic lines (L1, L2, L3 and L4). These lines expressed a combination of five transgenes, namely *Zmpsy1* (*Zea mays* phytoene synthase 1), *PacrtI* (*Pantoea ananatis* phytoene desaturase), *Gllycb* (*Gentiana lutea* lycopene β–cyclase), *Glbch* (*G. lutea* β–carotene hydroxylase) and *ParacrtW* (*Paracoccus* spp. β–carotene ketolase) (Table 1).

The key objective of these experiments was to ascertain the extent and impact of any interactions between the introduced transgenic pathway and the native carotenoid pathway during endosperm development. We determined the temporal profiles of mRNA and carotenoid accumulation, allowing us to reconstruct the corresponding enzyme activities, identify activities that were regulated transcriptionally and post-transcriptionally, and develop a theoretical model of the interactions allowing additional potential intervention points to be identified for targeted engineering of the carotenoid pathway. These potential interventions represent primary targets for engineering the maize endosperm carotenoid pathway in a more effective and predictable manner.

RESULTS

Analysis of transgene expression by quantitative real-time RT–PCR

We compared transgene expression levels in four maize genetic backgrounds at several endosperm developmental stages from 10 to 30 days after pollination (DAP; Figure 2). *Zmpsy1* transcript levels peaked between 20 and 25 DAP in lines 1, 3 and 4, but remained constant throughout the analysis period in line 2. *PacrtI* was expressed in all four transgenic lines, with line 3 showing the highest expression levels overall. The expression profile in line 3 peaked at 25 DAP and then decreased from 30 DAP onwards. *Gllycb* was expressed at similar levels in lines 2 and 3 and at higher levels in line 4 (Figure 2). The maximum expression was observed at 30 DAP in all four lines. *Glbch* was only expressed in line 4, peaking at 20 DAP. *ParacrtW* was expressed in lines 3 and 4. Expression was much higher in

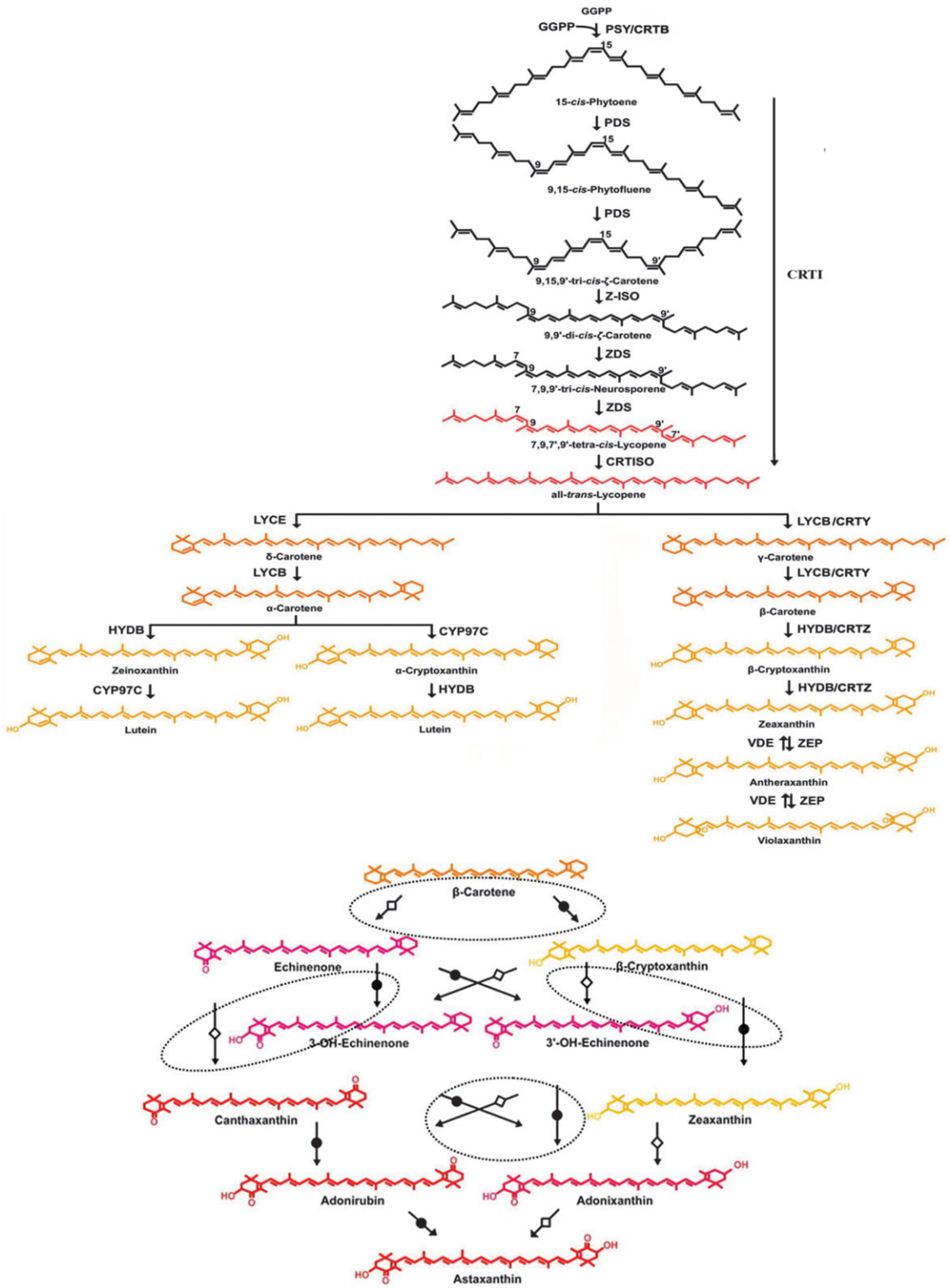

Figure 1. The extended carotenoid biosynthesis pathway in plants and equivalent steps in bacteria.
GGPP, geranylgeranyl diphosphate; GGPPS, GGPP synthase; PSY, phytoene synthase; PDS, phytoene desaturase; ZISO, ζ–carotene isomerase; ZDS, ζ–carotene desaturase; CRTISO, carotenoid isomerase; LYCB, lycopene β–cyclase; LYCE, lycopene ε–cyclase; CYP97C, carotene ε–ring hydroxylase; HYDB, β–carotene hydroxylase (BCH, CYP97A or CYP97B). Arrows with a white square in the middle indicate β–carotene ketolase (BKT, known in bacteria as CRTW or CRTO); arrows with a black circle in the middle indicate β–carotene hydroxylase (BCH or CRTZ) [11].

Table 1 Transgenic maize lines expressing *Zmpsy1* (*Zea mays* phytoene synthase 1), *Pacrtl* (*Pantoea ananatis* phytoene desaturase), *Gllycb* (*Gentiana lutea* lycopene β–cyclase), *Glbch* (*G. lutea* β–carotene hydroxylase) and *ParacrtW* (*Paracoccus* spp. β–carotene ketolase)

Line	Expressed genes
Line 1	*Zmpsy1* and *Pacrtl*
Line 2	*Zmpsy1*, *Pacrtl* and *Gllycb*
Line 3	*Zmpsy1*, *Pacrtl*, *Gllycb* and *ParacrtW*
Line 4	*Zmpsy1*, *Pacrtl*, *Gllycb*, *ParacrtW* and *Glbch*

line 3 and peaked at 25 DAP, whereas expression levels remained constant in line 4.

Analysis of endogenous gene expression by quantitative real-time RT–PCR

We also analyzed the expression of 12 endogenous carotenogenic genes (*Zmpsy2*, *Zmpds*, *Zmzds*, *Zmcrtiso*, *Zmlyce*, *Zmlycb*, *Zmbch1*, *Zmbch2*, *ZmCYP97A*, *ZmCYP97B* and *ZmCYP97C*) during endosperm development in the four transgenic lines and in wild-type plants (Figure 2). Quantitative real-time RT–PCR showed that *Zmpsy2* was expressed at low levels in all four lines and wild-type plants, whereas *Zmpds* and *Zmzds* were expressed at higher levels in the transgenic plants. There was little difference among the transgenic lines, and expression peaked at 30 DAP.

Zmcrtiso was also expressed at higher levels in the transgenic plants, although not to the degree seen with *Zmpds* and *Zmzds*. These genes were expressed more strongly in lines 2 and 3. *Zmlyce* was also induced in the transgenic plants and peaked at 30 DAP, but there were differences between lines earlier in development. In line 1, *Zmlyce* expression decreased from 15 to 25 DAP and then increased at 30 DAP, whereas in line 2, it was expressed at a constant level from 15 to 25 DAP, followed by an increase at day 30. Lines 3 and 4 showed the same expression pattern, i.e. increasing expression up to day 20, followed by a plateau and then a peak at 30 DAP. *Zmlycb* mRNA levels were similar in all plants, and peaked at 25 DAP.

Zmbch1 levels were similar to wild-type in all lines, whereas *Zmbch2* levels were higher in the transgenic lines, especially in line 1. *Zmbch2* expression in all lines peaked at 30 DAP except in line 3, where expression peaked at 25 DAP. Lines 1 and 4 showed the same *Zmbch2* expression profile, but the expression level in line 2 was lower. Line 1 showed the highest *Zmbch2* expression levels among all the lines, and expression increased during development until 30 DAP. The expression of *ZmCYP97A*, *ZmCYP97B* and *ZmCYP97C* peaked at 30 DAP in the transgenic lines, but the overall levels were much lower than in wild-type endosperm.

Carotenoid measurement, aggregate enzyme activities, and flux control by various genes

Carotenoid levels were measured between 15 and 60 DAP, and we found that carotenoids were synthesized continuously in the endosperm from 15 DAP onwards. A detailed description of the carotenoid extraction, separation and identification procedure is provided in Methods S1. The concentration of most carotenoids peaked during development and then decreased as the seeds matured, with only β–cryptoxanthin, α–cryptoxanthin and echinenone continuing to accumulate up to 60 DAP (Table 2). The levels of some carotenoids decreased marginally after peaking (e.g. lutein), whereas others decreased significantly (e.g. antheraxanthin).

We interpolated the carotenoid levels for the days between experimental measurements, providing us with an extended experimental time series that allowed us to estimate time-dependent aggregate enzyme activities to explain the time course of the metabolites in each line. Because we calculated the activities at each time point, any regulatory interactions that may modulate those activities are implicitly considered. The estimate involved fitting an ordinary differential equation system written in mass action form (Alves *et al.*, 2008). The rate parameters of the system were estimated independently at each time point in order to predict the rate constant for the production and consumption flux of each variable (Figure 3).

The predicted enzyme activities are the aggregate of several individual enzymes that catalyze biosynthesis reactions, and we were able to combine these data with the transcript profiles to determine whether the gene expression profiles correlated with the aggregated enzyme activities and explained their variation. If this correlation exists and is statistically significant, the most parsimonious interpretation is that changes in enzyme activity are regulated at the level of transcription, and transcript abundance therefore modulates the relevant aggregate enzyme activity. If no correlation is found, the data are consistent with post-translational regulation, because the proteins encoded by the relevant genes are responsible for the synthesis and degradation of the various carotenoid metabolites. If there are changes in the amount of these metabolites between the various maize lines and these changes cannot be explained by variations in gene expression, metabolite variation must be a cosequence of changes in mRNA degradation, enzyme synthesis and/or enzyme activity. Finally, if there is correlation but not enough to explain the observed variation, we may estimate how much each gene contributes to the changes in the aggregate enzyme activity.

The results are presented in Tables S1 and S2. The R^2 values were significant ($P < 0.01$) according to an *F*–test of the linear models used to calculate how much of the

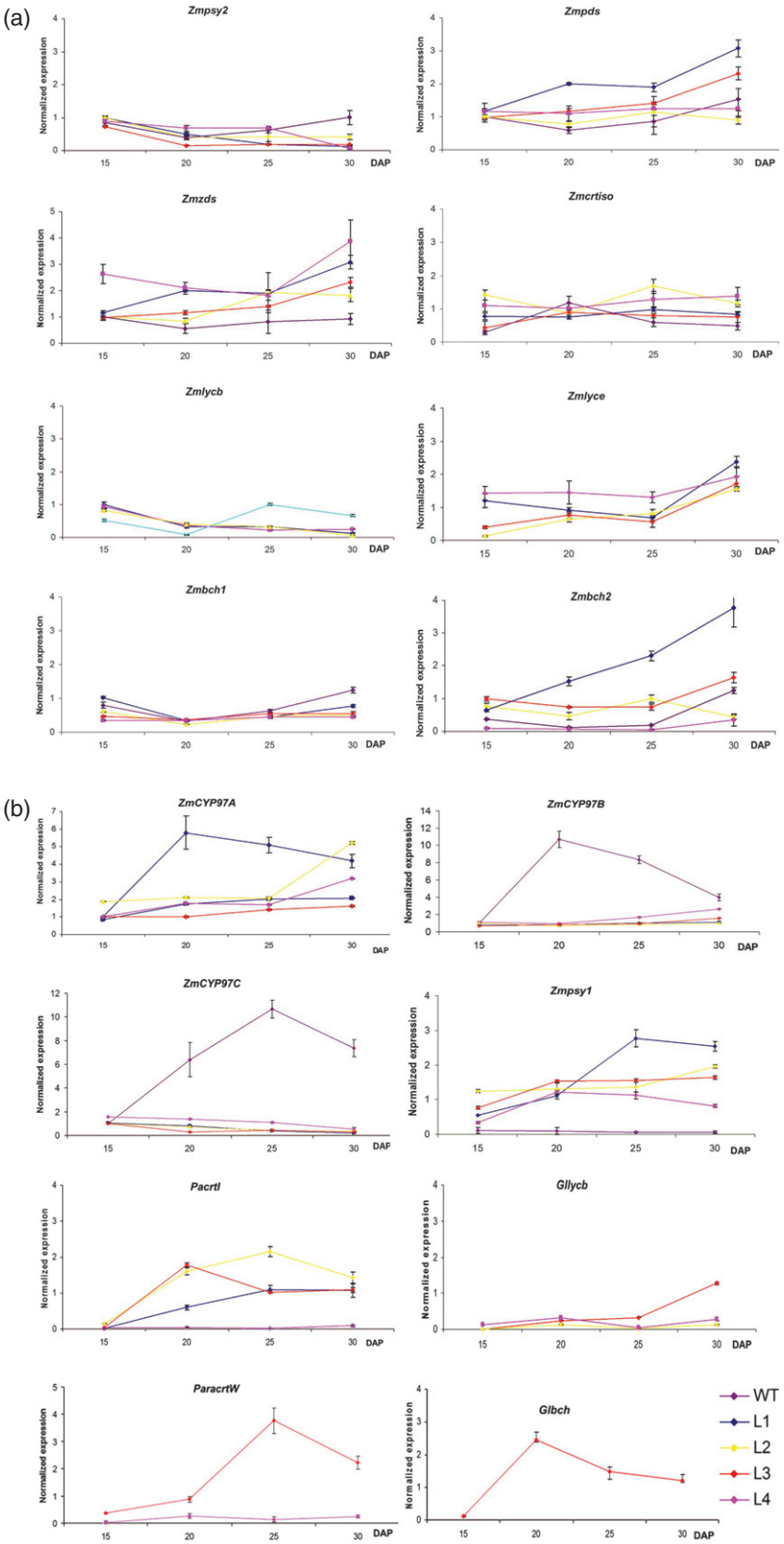

Figure 2. Quantitative real-time RT–PCR analysis of carotenogenic endogenous genes and transgenes in transgenic maize plants compared to the wild-type control (a, b). Data represent relative mRNA levels in the immature maize endosperm of wild-type plants and four transgenic lines (L1, L2, L3 and L4) at four developmental stages (15, 20, 25 and 30 DAP), normalized against actin mRNA and presented as the mean of three replicates SD.
Zm, *Zea mays*; Pa, *Pantoea annatis*; GI, *Gentanua lutea*; Para, *Paracoccus*; PSY1/2, phytoene synthase 1/2; PDS, phytoene desaturase; ZDS, ζ–carotene desaturase; CRTISO, carotene isomerase; LYCB, lycopene β–cyclase; LYCE, lycopene ε–cyclase; BCH1/2, β–carotene hydroxylase 1/2; CYP97A, carotene ε–hydroxylase; CYP97C; ZEP2, zeaxanthin epoxidase 2.

Table 2 Time of maximum accumulation of various carotenoids in the four transgenic lines (days after pollination)

Carotenoid	Line 1	Line 2	Line 3	Line 4	M37W
Phytoene	50	40–50	50	40	–
Lycopene	50	0	40–50	–	–
β–carotene	30–50	40	50	30–40	–
α–carotene	–	–	50	30–50	–
β–cryptoxanthin	25–30	40	40–60	25–60	–
α–cryptoxanthin	25–40	40	40–60	50	–
Lutein	30–40	30–40	30–40	50	30–40
Zeaxanthin	25–30	25	25–30	30–50	30
Antheraxanthin	20–25	25	20	25	–
Echinenone	–	–	40–50	30–60	–
3–hydroxyechinenone	–	–	30–50	20	–
Adonixanthin	–	–	40	25	–
Astaxanthin	–	–	25	–	–
Total	30–50	40	30–40	30–40	30–40

changes in predicted enzyme activity may be justified by changes in gene expression. The initial predicted aggregate enzyme activity required for the production of phytoene was found to be similar in lines 1–3 but much higher in line 4. Between days 25 and 40, this activity was predicted to be approximately constant in lines 1, 3 and 4, but decreasing in line 2. After day 40, lines 2 and 3 were predicted to produce less phytoene than lines 1 and 4. These dynamic changes in predicted enzyme activity correlated well with the gene expression profile for *PSY1* in lines 2 and 4. *PSY1* explained more than 60% of the changes in both lines. The changes in gene expression observed in lines 1 and 3 explained <30% of the changes in phytoene production.

In summary, these results suggest that phytoene production is regulated mostly at the level of gene expression in lines 2 and 4, with *PSY1* providing the greatest contribution. On the other hand, our results are consistent with phytoene production in lines 1 and 3 being regulated both transcriptionally and post-transcriptionally.

The aggregate enzyme activity responsible for flux entry into the α–branch was quite low. This flux was predicted to be approximately the same in lines 2, 3 and 4 after day 20, and was slightly higher in line 1. Approximately 73% of the dynamic changes in this activity were explained by changes in *LYCE* gene expression in line 1. In line 2, the correlation between changes in gene expression and changes in aggregate enzyme activity was non-significant. In lines 3 and 4, respectively, 39 and 58% of the variation in aggregate enzyme activity was explained by changes in the expression of *Gllycb*. These scenarios are consistent with either an important role for post-transcriptional regulation of flux or the possibility that several genes contribute to the flux at significant levels.

The aggregate enzyme activity responsible for flux entry into the β–branch was predicted to be more than twice that for flux entry into the α–branch. However, significant correlations between changes in gene expression and changes in this activity were only found for lines 3 and 4. In these lines, variation in *Gllycb* explained 32 and 56% of the variations in flux, respectively.

In summary, these results suggest that material flux into the pathway is regulated mostly at the level of gene expression in lines 2 and 4, and both transcriptionally and post-transcriptionally in lines 1 and 3. In contrast, flux into the branch points appears to be regulated mostly at the post-transcriptional level.

In lines 3 and 4, flux may be diverted from the β–branch to the echinone route. Changes in the expression of *ParacrtW* explained 48–86% of the changes in the various enzyme activities that contribute to this flux in line 3. In contrast, in line 4, variations in the expression of *ParacrtW* explained only a small fraction of the changes in aggregate enzyme activity. This is consistent with predominant transcriptional regulation for this enzyme activity in line 3 and post-transcriptional regulation in line 4.

The aggregate enzyme activity responsible for the production of antheraxanthin was explained by variation in the expression of *ZEP2* in line 2, consistent with a predominance of transcriptional regulation. In all other lines, post-transcriptional regulation appeared to play an important role in regulating this activity.

Carotene accumulation during endosperm development

Phytoene began to accumulate at 15 DAP in line 3, and later in lines 1, 2 and 4, peaking at 40–50 DAP (Figure 4a). The lowest phytoene concentration was detected in line 4 (13.88 ± 0.67 μg g^{-1} dry weight, DW). Lycopene was only detected in lines 1 and 3. Lycopene began to accumulate by 15–20 DAP in both lines. The most significant increase in lycopene was observed between 20 and 25 DAP in line 3, followed by a marginal increase to the maximum at 40–50 DAP and a decrease towards 60 DAP, whereas in line 1, lycopene increased between 15 and 20 DAP, then reached a plateau between 20 and 25 DAP, followed by another increase up to 30 DAP and continued accumulation up to day 50 (Figure 4b). The highest concentration of lycopene was detected in line 3, followed by line 1 (6.25 ± 0.22 and 3.72 ± 0.41 μg g^{-1} DW, respectively).

Line 4 contained the highest concentration of β–carotene, followed by lines 1, 2 and 3 (26.33 ± 0.15, 13.62 ± 0.45, 5.36 ± 0.14 and 5.34 ± 0.33 μg g^{-1} DW, respectively). Accumulation of β–carotene began by 15 DAP in line 1, but between 15 and 20 DAP in lines 3 and 4 and after day 20 in line 2, reaching maximum levels between 30 and 60 DAP depending on the line (Figure 4c). α–carotene was only detected in line 4 and at low levels (0.91 ± 0.03 μg g^{-1} DW). In addition, α–carotene accumulation began later than that of other carotenoids.

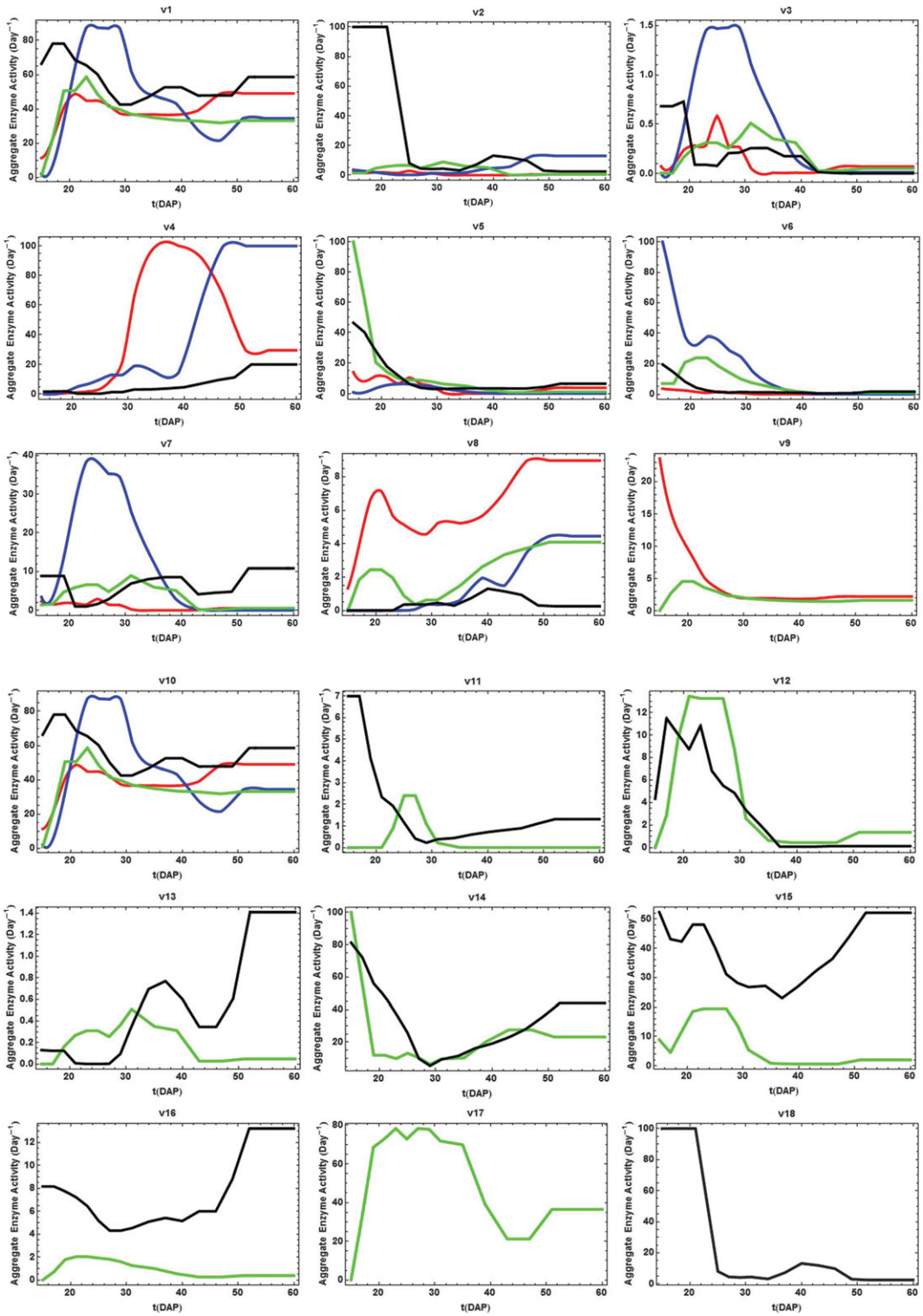

Figure 3. Predicted aggregate enzyme activity for the reactions in Figure 2.
Red, line 1; blue, line 2; green, line 3; black, line 4.

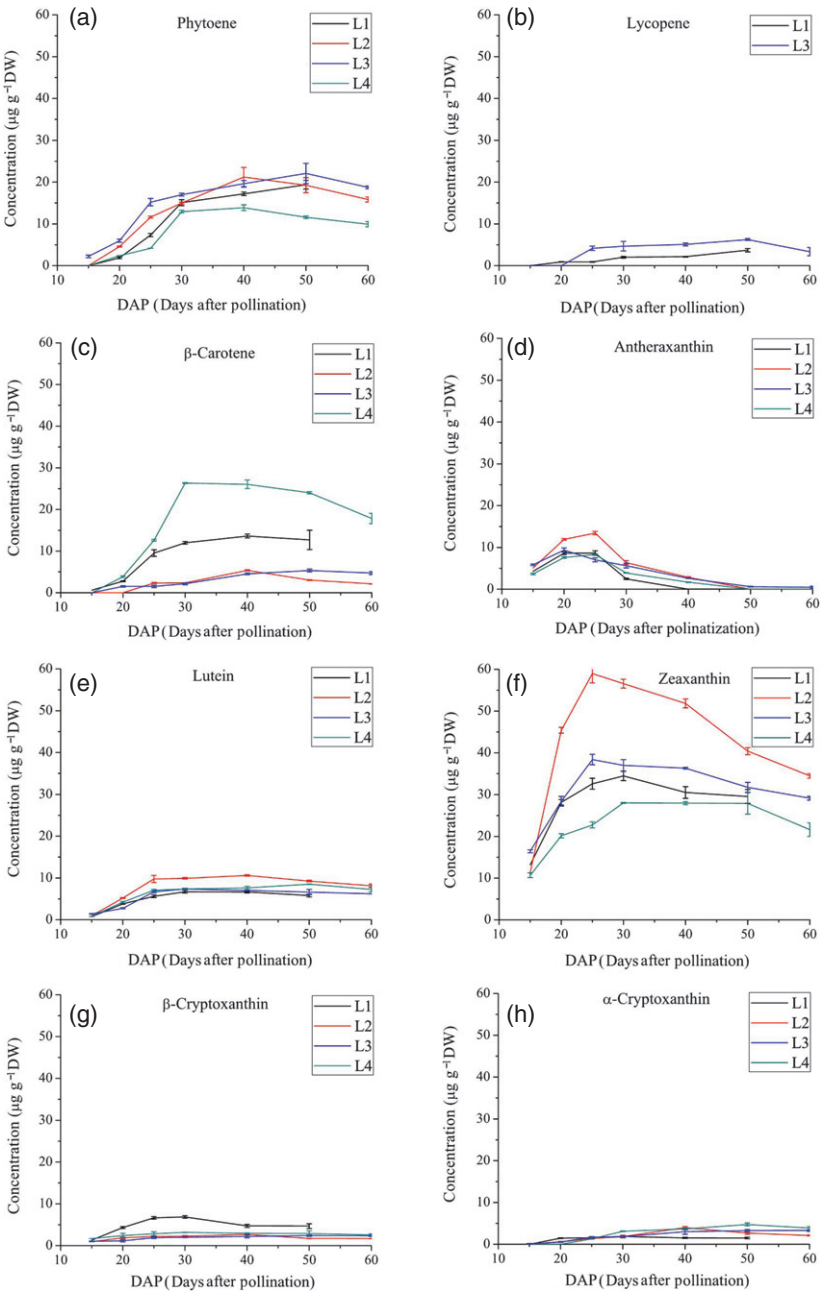

Figure 4. Total and individual carotenoid concentration profiles during maize endosperm development.
(a) Phytoene, (b) lycopene, (c) β–carotene, (d) antheraxanthin, (e) lutein, (f) zeaxanthin, (g) β–cryptoxanthin, (h) α–cryptoxanthin, (i) adonixanthin, (j) 3–hydroxyechinenone, (k) echinenone, (l) astaxanthin, (m) total ketocarotenoid content and (n) total carotenoid content in μg per g dry weight (DW).

Xanthophyll accumulation during endosperm development

The profile of antheraxanthin accumulation was similar in all lines, and the highest levels were detected in line 2 (Figure 4d). Antheraxanthin began to accumulate by 15 DAP, peaked at 20–25 DAP (depending on the line), and rapidly decreased to undetectable levels thereafter, the most dramatic loss among all the carotenoids we measured. This behavior may indicate that antheraxanthin is more reactive than other carotenoids due to the presence of an epoxy group, or may reflect its status as a precursor of abscisic acid.

The lutein profile was similar in all the transgenic lines (Figure 4e), increasing steadily and peaking by 30–40 DAP (lines 1, 2 and 3) or 50 DAP (line 4), before decreasing slightly. The highest level of lutein was detected in line 2, followed by lines 4, 3 and 1 (10.59 ± 0.17, 8.51 ± 0.02, 7.35 ± 0.17 and 6.70 ± 0.33 μg g^{-1} DW, respectively). Zeaxanthin was the major carotenoid found in all four lines (39.92, 49.65, 32.95 and 28.18% of total carotenoid concentration at 30, 40, 40 and 30 DAP, in lines 1, 2, 3 and 4,

Figure 4. continued

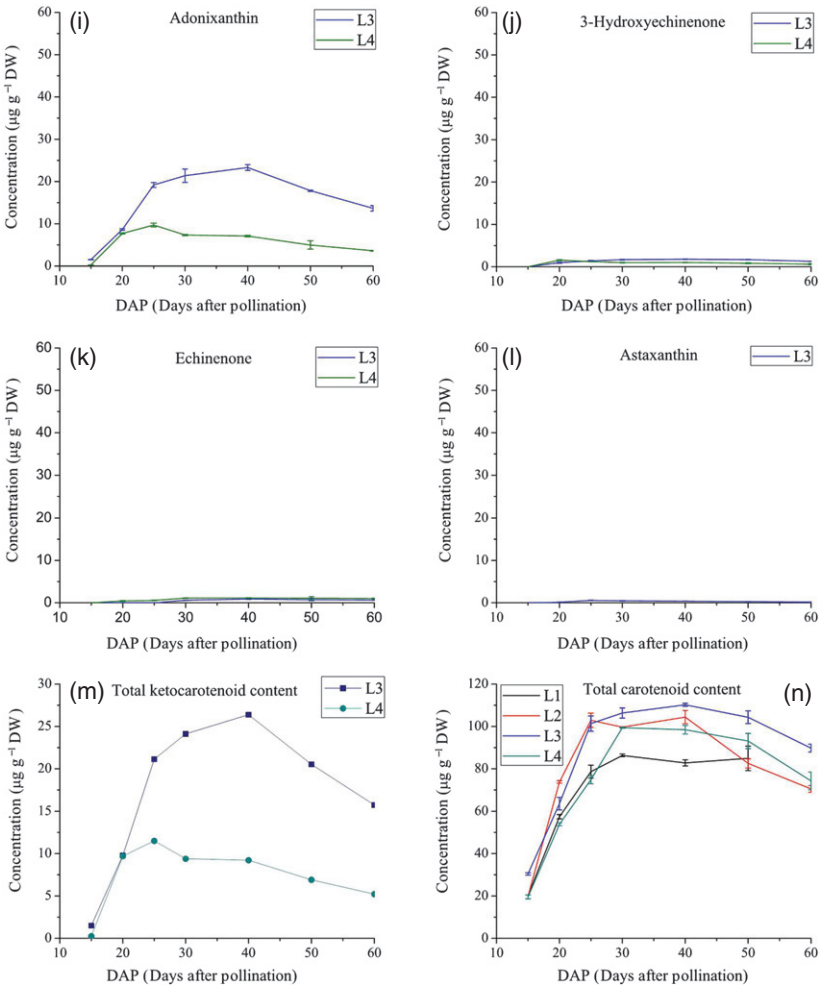

respectively; Figure 4f). Accumulation began by 15 DAP, and increased steadily until 25–30 DAP in lines 1 and 3, 25 DAP in line 2 and 30–50 DAP in line 4. The accumulation of β–cryptoxanthin was similar in lines 2, 3 and 4, but the peak accumulation was higher and earlier in line 1 (Figure 4g), and there was no decrease from the peak in lines 3 and 4. The maximum concentration of α–cryptoxanthin was found by 25–40, 40, 40–60 and 50 DAP in lines 1, 2, 3 and 4, respectively, followed by a decrease in all lines except line 3 (Figure 4h).

Individual and total ketocarotenoid accumulation during endosperm development

Ketocarotenoids were only detected in lines 3 and 4, reflecting the expression of *ParacrtW* in addition to *Zmpsy1*, *Pacrtl* and *Gllycb* (line 3) or *Zmpsy1*, *Pacrtl*, *Gllycb* and *Glbch* (line 4). The most abundant ketocarotenoid in both lines was adonixanthin (Figure 4i). In line 3, adonixanthin levels increased significantly between 15 and 25 DAP, then more moderately until 40 DAP before decreasing. In contrast, adonixanthin levels in line 4 increased significantly between 15 and 20 DAP, peaking at 25 DAP and then decreasing. We also detected 3–hydroxyechinenone and echinenone in lines 3 and 4 but at much lower concentrations than adonixanthin (Figure 4j,k). Echinenone accumulation began after 15 DAP in line 4 but after 25 DAP in line 3, increasing to a maximum at 40–50 and 30–60 DAP in lines 3 and 4, respectively, and decreasing only in line 3 (Figure 4k). The maximum echinenone concentration was similar for both lines, whereas adonixanthin levels were higher in line 3 than line 4. Similarly, the highest levels of 3–hydroxyechinenone were found in line 3, where the concentration increased steadily and peaked at 30–50 DAP compared to the earlier peak at 20 DAP in line 4 (Figure 4j). In both lines, the 3–hydroxyechinenone level decreased after reaching its maximum concentration. Astaxanthin was only detected in line 3 at low levels, starting at 15 DAP and increasing between 20 and 25 DAP before decreasing (Figure 4l). Line 3 accumulated the highest total ketocarotenoid levels (up to 26 μg g^{-1} DW, starting at 15 DAP; Figure 4m). Total ketocarotenoids increased most significantly between 15 and 25

DAP in line 3 and between 15 and 20 DAP in line 4, then more moderately to a peak at 40 DAP in line 3 and at 25 DAP in line 4 before decreasing.

Total carotenoid accumulation during endosperm development

Although individual carotenoid concentrations peaked on different days after pollination, the total carotenoid content peaked between 30 and 40 DAP in all lines (Figure 4n). The total carotenoid levels in lines 1, 2 and 4 were similar at 15 DAP, but there was higher accumulation in line 3. The most significant increase in total carotenoid levels took place between 15 and 25 DAP in lines 1, 2 and 3 but between 15 and 30 DAP in line 4. There was a further slight increase in lines 1, 3 and 4 until the maximum, whereas there was a small dip in concentration between 25 and 30 DAP in line 2. The maximum total carotenoid content in line 1 was observed at 30–50 DAP (86.34 ± 0.65 μg g^{-1} DW), whereas in line 2 the maximum occurred at 40 DAP (104.4 ± 3.08 μg g^{-1} DW), and in lines 3 and 4 it occurred at 30–40 DAP (110.21 ± 0.72 and 99.42 ± 0.27 μg g^{-1} DW, respectively). Total carotenoids then decreased in lines 2, 3 and 4. The highest overall total carotenoid content was observed in line 3 (Figure 5), which expressed *Zmpsy1*, *Pacrtl*, *Gllycb* and *ParacrtW*. The total carotenoid content in wild-type M37W was 1.10 μg g^{-1} DW (Figure 5). Thus, carotenoid content was increased 78.5-, 94.9-, 100.2- and 90.4-fold, respectively, in lines 1, 2, 3 and 4.

DISCUSSION

Regulation of carotenoid biosynthesis in plants

The enzymes required for plant carotenoid biosynthesis are encoded by nuclear genes and targeted to the plastids (Bartley and Scolnik, 1994). In starchy maize kernels, carotenoids accumulate predominantly in endosperm tissue (Steenbock and Coward, 1927; Blessin *et al.*, 1963), particularly in amyloplasts, where they play an important role in abscisic acid production and seed dormancy (Maluf *et al.*, 1997).

Most of the genes encoding carotenogenic enzymes in plants have been identified and functionally characterized (Farré *et al.*, 2009; Li *et al.*, 2010). The regulation of carotenoid biosynthesis is complex and is restricted to specific tissues (Lima *et al.*, 2005). It therefore requires comprehensive understanding of gene regulation, biochemical interactions among the enzyme complexes, and the interconversion of metabolites (Taylor and Ramsay, 2005). Carotenoid accumulation in seeds, fruits and flowers correlates with the abundance of transcripts representing key carotenoid genes (Fraser *et al.*, 1994; Zhu *et al.*, 2010). A positive correlation between higher *psy1* transcript levels and enzyme activity was observed in tomato (*Solanum lycopersicum*), increasing the carotenoid content in the ripened fruit (Fraser *et al.*, 1994). The accumulation of high levels of lycopene in tomato fruit suggests that a different regulatory mechanism may be involved in carotenogenesis in green tissues, which accumulate less lycopene (Fraser *et al.*, 1994). A similar positive correlation was observed in carrot (*Daucus carota*) transformed with *psy1*, resulting in a 93-fold increase in total carotenoids (Maass *et al.*, 2009). A negative correlation between higher zeaxanthin epoxidase (*zep*) transcript levels and zeaxanthin levels was observed in potato tubers by silencing the endogenous *zep* gene (Romer *et al.*, 2002).

Phytoene synthesis

Phytoene synthase (PSY) is the first committed enzyme in carotenoid biosynthesis, and has been extensively studied in maize because it is rate-limiting for production of carotenoids in the endosperm (Gallagher *et al.*, 2004; Wong

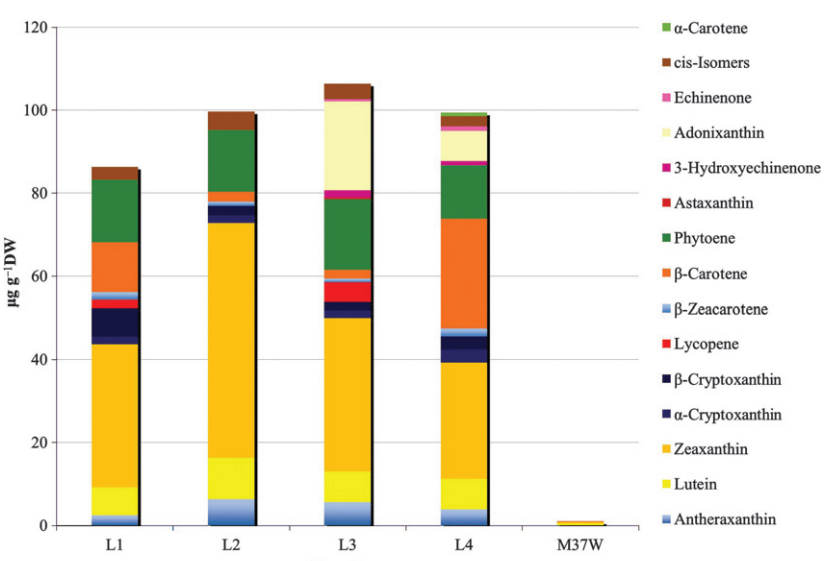

Figure 5. Carotenoid composition at 30 days after pollination in the four transgenic lines.
Line 1 expresses *Zmpsy1* and *Pacrtl*; line 2 expresses *Zmpsy1*, *Pacrtl* and *Gllycb*; line 3 expresses *Zmpsy1*, *Pacrtl*, *Gllycb* and *ParacrtW*; line 4 expresses *Zmpsy1*, *Pacrtl*, *Gllycb*, *ParacrtW* and *Glbch*.

et al., 2004; Pozniak *et al.*, 2007; Li *et al.*, 2008; Zhu *et al.*, 2008). Maize, like other grasses, has multiple genes encoding PSY, but only *psy1* transcript levels correlate with carotenoid levels in the endosperm (Buckner *et al.*, 1996). The *psy2* transcript is mainly expressed in leaves and at lower levels in embryos (Gallagher *et al.*, 2004). The *psy3* transcript is expressed predominantly in the root and embryo (Li *et al.*, 2008). These expression profiles suggest that maize PSY genes may be functionally specific rather than redundant (Li *et al.*, 2009).

Our analysis of mRNA levels revealed that the *Zmpsy1* transcript is present at low levels in M37W endosperm, whereas all the transgenic lines expressed the transcript strongly. *Zmpsy2* expression as determined by quantitative real-time RT–PCR suggested that the residual carotenoid content of M37W endosperm may reflect the activity of PSY2. Although *Zmpsy2* transcripts were detected in M37W endosperm, the total carotenoid content remained low, confirming that PSY1 rather than PSY2 plays a crucial role in carotenoid accumulation in the endosperm.

When we integrated the results from our RNA and metabolic analysis in transgenic lines 1–4, we found that PSY1 rather than PSY2 appears to be responsible for most phytoene production. The results are also consistent with phytoene production being regulated mostly at the level of gene expression in lines 2 and 4, but both transcriptionally and post-transcriptionally in lines 1 and 3. Thus, PSY1 appears to be the preferred choice for designing a pathway with more efficient phytoene production (first organization principle).

Phytoene desaturation and isomerization

We found that the phytoene desaturase (*Zmpds*), ζ–carotene desaturase (*Zmzds*) and carotene isomerase (*Zmcrtiso*) transcripts were present at similar levels in all lines, although *Zmpds* and *Zmzds* mRNAs were more abundant than *Zmcrtiso* mRNAs. The expression of *Pacrtl* increased the lycopene content in lines 1 and 3. However, phytoene was detected in all lines, suggesting that the desaturation steps may be rate-limiting. The *Pacrtl* and *Zmcrtiso* mRNAs were most abundant in line 3, consistent with the higher accumulation of lycopene in this line. Phytoene was not detected in wild-type M37W endosperm but accumulated in all of the transgenic lines. Our estimation of aggregate enzyme activities for transformation of phytoene into lycopene indicated that this activity is 4–10 times lower than the aggregate enzyme activity for production of phytoene (compare panels v9 and v10 in Figure 3). Taken together, these observations suggest that the conversion of phytoene to lycopene (catalyzed by both endogenous desaturases/isomerases and *Pacrtl*) is a rate-limiting step for carotenoid biosynthesis in the transgenic lines. This suggests a second organization principle for designing more efficient pathways, i.e. modifying maize lines using genes that effectively convert phytoene to lycopene.

Lycopene cyclization

Higher levels of lycopene accumulate in lines 1 and 3, but no lycopene was detected in lines 2 and 4. The aggregate enzyme activity responsible for the production of lycopene is shown in panel v9 in Figure 3, while the aggregate enzyme activities for production of β- and α–branch metabolites are shown in panels v1 and v5, respectively. Because no lycopene is detected in lines 2 and 4, the ratio (panel v9)/(panels v1 + v5) is much lower than in line 1. In lines 1 and 3, this ratio is always lower than 0.5. Together, these observations indicate that production of lycopene is rate-limiting for the production of metabolites in the two lower branches of the pathway. Our analysis of the Granger causality between changes in gene expression and changes in metabolite levels indicates that changes in lycopene consumption may be explained almost entirely by the changes in gene expression in the various lines. In turn, this suggests that post-transcriptional regulation plays a small role in regulating lycopene production and utilization. Line 4 expressed *Gllycb* at the highest levels and contained more β–carotene. The β:α ratio was 6.37 in line 1 (*Zmpsy1* + *Pacrtl*), 5.85 in line 2 (*Zmpsy1* + *Pacrtl* + *Gllycb*), 7.83 in line 3 (*Zmpsy1* + *Pacrtl* + *Gllycb* + *ParacrtW*) and 6.39 in line 4 (*Zmpsy1* + *Pacrtl* + *Gllycb* + *ParacrtW* + *Glbch*) at 30 DAP. As observed in transgenic canola (Ravanello *et al.*, 2003) and rice (*Oryza sativa*) (Ye *et al.*, 2000), the β–branch of the pathway appears to be favored in maize.

Hydroxylation

Hydroxylation of the β- and ε–rings is performed by β–hydroxylase and ε–hydroxylase, respectively (Pogson *et al.*, 1996; Hirschberg, 2001). Following gene duplication and divergence, many plants have multiple β–carotene hydroxylases, including Arabidopsis (Rissler and Pogson, 2001), tomato (Liu *et al.*, 2003), saffron (*Crocus sativus;* Castillo *et al.*, 2005) and maize (Li *et al.*, 2010). We observed low levels of *Zmbch1* in all lines and higher levels of *Zmbch2*, with particularly high levels in line 1, correlating with higher levels of zeaxanthin. The higher levels of hydroxylated products (such as lutein and zeaxanthin) and lower levels of β–carotene in lines 1, 2 and 3 indicated efficient hydroxylation of α- and β–carotenes. In line 2, the low levels of β–carotene and higher levels of zeaxanthin appear to reflect the high levels of *Zmbch2* mRNA and the lower levels of *ZmCYP97C* mRNA, as suggested by Granger causality analysis (Table S2).

Ketolation

The carotenoid pathway may be extended to include ketocarotenoids such as astaxanthin by expressing *ParacrtW*.

This was expressed together with *Zmpsy1*, *PacrtI* and *GIlycb* in lines 3 and 4, with the latter also expressing *GIbch*. This led to the synthesis of adonixanthin, echinenone (4–keto-β–carotene) and 3–hydroxyechinenone in line 4, and these three carotenoids plus astaxanthin (3,3′–dihydroxy-4,4′–diketo-β–carotene) in line 3. Line 4 has a genotype similar to that of line 2, with additional *GIbch* and *ParacrtW* genes, and accumulated mainly β–carotene and zeaxanthin in addition to the ketocarotenoids.

Astaxanthin is formed from β–carotene by the addition of keto groups at the 4 and 4′ positions and hydroxyl groups at the 3 and 3′ positions of the β–ionone rings. These reactions are catalyzed by β–carotene ketolase and β–carotene hydroxylase, respectively. Each enzyme may perform its reaction independently, but further events depend critically on which reaction occurs first (Fraser *et al.*, 1997). *Paracoccus* β–carotene ketolase has a strong preference for carotenoids with at least one non-hydroxylated β–ionone ring, e.g. β–carotene, β–cryptoxanthin, echinenone and 3–hydroxy-echinenone, whereas 3–hydroxylated β–ionone rings such zeaxanthin, 3′–hydroxy-echinenone and adonixanthin are poor substrates for this enzyme (Fraser *et al.*, 1998).

The ketolase CRTW uses the same substrate as β–carotene hydroxylase, i.e. an unsubstituted β–ionone ring. The hydroxylase and ketolase thus compete at four steps for substrates in the extended carotenoid pathway: for β–carotene, the unsubstituted site of β–cryptoxanthin, echinenone and 3–hydroxyechinenone (Figure 1). In general, non-ketolated zeaxanthin, the mono-keto derivative 3′–hydroxy-echinenone and the dihydroxy-monoketocarotenoid adonixanthin represent alternative intermediates in the pathway to astaxanthin. Thus, astaxanthin in maize endosperm may be preferentially derived from echinenone via either 3–hydroxy-echinenone or canthaxanthin and then adonirubin.

Because the 3–hydroxylated β–ionone ring is poorly ketolated (Fraser *et al.*, 1998), the ketolase must compete with the hydroxylase twice (first during ketolation of β–carotene, then during ketolation of either echinenone or 3–hydroxyechinenone), and succeed each time or astaxanthin is not formed. Therefore, the accumulation of astaxanthin is determined by the abundance of the ketolase relative to the hydroxylase. Only plants expressing *ParacrtW* produce enough ketolase to ensure the formation of astaxanthin. Otherwise, adonixanthin is the final keto-hydroxy product of the pathway. This appears to be the case in line 4, where total concentrations of ketolated carotenoids are much lower than in line 3, and the pathway stops without the second ketolation at the level of adonixanthin. Line 4, which expresses *GIbch* and *ParacrtW* in addition to other transgenes, did not accumulate astaxanthin due to the relatively high hydroxylase activity (i.e. the additional BCH activity due to expression of *GIbch* in line 4 but not in line 3). Line 3 accumulated the highest ketocarotenoid levels and was the only line able to synthesize astaxanthin, probably reflecting the relatively low hydroxylase activity (no BCH activity) and high ketolase activity (high CRTW activity).

For many plants transformed with a ketolase gene such as *ParacrtW* (Zhu *et al.*, 2009), conversion of adonixanthin to astaxanthin appears to be an important limiting step in astaxanthin biosynthesis. Astaxanthin and several ketocarotenoid intermediates involved in the formation of astaxanthin, including adonirubin, canthaxanthin, echinenone and adonixanthin, were detected in carrot tissues expressing an *Haematococcus pluvialis bkt* gene, and heterologous expression of BCH was not required for ketocarotenoid synthesis due to up-regulation of endogenous hydroxylases in transgenic leaves and roots (Jayaraj *et al.*, 2008). Canola was transformed with *crt*Z (BCH) and *crt*W from the marine bacterium *Brevundimonas* SD212, as well as the *Paracoccus* N81106 *ipi* gene and the general carotenogenic genes *crt*E, *crt*B, *crt*I and *crt*Y from *Pantoea ananatis*, and plants expressing all seven genes accumulated 18.6 times more total carotenoids than wild-type plants, including ketocarotenoids such as echinenone, canthaxanthin, astaxanthin and adonixanthin, which were not found in wild-type seeds (Fujisawa *et al.*, 2009). However, adonixanthin levels were higher than those for astaxanthin. Comparing panels v14, v15 and v16 in Figure 3 shows that the aggregate enzyme activity for the production of astaxanthin (panel v16) is lower than that for the other steps of the pathway, reinforcing the hypothesis that this step is rate-limiting for astaxanthin biosynthesis. Furthermore, comparing panels v11–v13 in Figure 3 (conversion fluxes between the zeaxanthin and astaxanthin branches) with panels v3, v6 and v7 (zeaxanthin branch) and v14–v16 (astaxanthin branch) indicates that predicted aggregate enzyme activities in panels v11–v13 are up to an order of magnitude lower than those for the later reactions. Taken together, these observations imply that metabolite entry into the astaxanthin branch occurs at a lower rate than the reactions within each branch.

Transcript and carotenoid levels in various maize genetic backgrounds during endosperm development

All four transgenic lines exhibited similar transgene transcript levels, which increased during endosperm development and peaked at 20–25 DAP. However, *GIlycb* reached a maximum at 30 DAP, and this may explain why β–carotene levels peaked 30–50 DAP, depending on the line. Endosperm-specific promoters were used for all transgenes, and transgene expression had generally commenced by 15–20 DAP. Endogenous gene expression varied considerably, with some transcripts expressed at constant levels throughout development (*ZmCYP97B*, *ZmCYP97C* and *Zmpsy2*). Other transcripts increased gradually up to a

peak level at 30 DAP (*Zmpds*, *Zmzds*, *Zmlyce*, *Zmbch2* and *ZmCYP97A*) and others reached an earlier peak followed by a decrease (*Zmlycb*, *Zmbch1* and *Zmcrtiso*).

Individual carotenoids peaked at different stages of endosperm development from 15 to 60 DAP (Table 2). The early carotenoids (phytoene and lycopene) peaked at later stages (40–50 DAP), suggesting that they are consumed during early development to produce downstream carotenoids. Similarly, antheraxanthin accumulated before its precursor zeaxanthin, which in turn accumulated before its precursors in all lines (Table 2). However, the maximum accumulation of β–carotene and β–cryptoxanthin was specific to each transgenic line. In lines 1 and 2, which did not express hydroxylase or ketolase transgenes, the end products accumulated before the precursors as discussed above (zeaxanthin followed by β–cryptoxanthin and finally β–carotene). Line 3 accumulated astaxanthin, followed by adonixanthin and zeaxanthin, and then the precursors of those metabolites (3–hydroxyechinenone, echinenone, β–cryptoxanthin and β–carotene, respectively). The same behavior was observed in line 4, although with no astaxanthin accumulation due to the low ketolase activity compared with hydroxylases.

CONCLUSIONS

Important advances have been made in the characterization of many of the genes encoding enzymes in the carotenoid biosynthesis pathway. However, the regulatory mechanisms controlling carotenoid biosynthesis in maize endosperm are still unclear. A comparative investigation in various genetic backgrounds focusing on targeted carotenoid transcript and metabolite analysis allowed multiple bottlenecks to be identified in the pathway. Quantitative real-time RT–PCR revealed the near absence of *Zmpsy1* transcripts in M37W endosperm as expected, whereas *Zmpsy2* transcripts were present, suggesting that the residual carotenoid content most likely reflects the activity of PSY2. The conversion of phytoene to lycopene (catalyzed by both endogenous desaturases/isomerases and *Pacrtl*) is a rate-limiting step for carotenoid biosynthesis in the transgenic lines because phytoene was still detected in all lines. In many plants transformed with a ketolase gene, such as *ParacrtW*, the conversion of adonixanthin to astaxanthin appears to be an important limiting step for astaxanthin biosynthesis. Our results are consistent with this, confirming that adonixanthin accumulation must be avoided to achieve the production of astaxanthin in transgenic maize endosperm. The accumulation profiles of individual carotenoids indicate that, although carotenoid synthesis starts at the earliest stages of endosperm development, their accumulation is likely to depend on feedback regulatory loops. The accumulation of β–carotene cannot begin any earlier than that of zeaxanthin because the intermediate is initially consumed to make end products, such as zeaxanthin or various ketocarotenoids depending on the line. This behavior was observed for almost all the carotenoid precursors and end products. The identification of a number of further bottlenecks and rate-limiting steps in the pathway provides data for further investigations to ascertain in more detail the genetic and molecular factors that influence carotenoid content and composition in various maize genetic backgrounds, and for future biofortification strategies that aim to increase particular carotenoids in maize endosperm.

Table 3 Primer sequences for the amplification of the maize *actin* gene (for normalization) and the endogenous and heterologous carotenogenic genes by quantitative real-time RT–PCR

Gene	Forward primer	Reverse primer
Zmpsy1	5′-CATCTTCAAAGGGGTCGTCA-3′	5′-CAGGATCTGCCTGTACAACA-3′
Zmpsy2	5′-TCACCCATCTCGACTCTGCTA-3′	5′-GATGTGATCTACGGATGGTTCAT-3′
Zmpds	5′-TGTTTGTGCAACACCAGTCG-3′	5′-CTCCTGCTGAAAAGAAGGTGG-3′
Zmzds	5′-GAATGGAGGGAGTGGGAAATG-3′	5′-AGTCTGCATCCGCCGTGTAC-3′
Zmcrtiso	5′-GAATTATATGATTACGGTGTCAGG-3′	5′-TGAAGGGTATCTCAAAACAGAACT-3′
Zmlyce	5′-TTTACGTGCAAATGCAGTCAA-3′	5′-TGACTCTGAAGCTAGAGAAAG-3′
Zmlycb	5′-GACGCCATCGTAAGGTTCCTC-3′	5′-TCGAGGTCCAGCTTGAGCAG-3′
Zmbch1	5′-CCACGACCAGAACCTCCAGA-3′	5′-CATGGCACCAGACATCTCCA-3′
Zmbch2	5′-GCGTCCAGTTGTATGCGTTGT-3′	5′-CATCTATCGCCATCTTCCTTT-3′
ZmCYP97A	5′-CTGGAGCCATCTGAAAGTCA-3′	5′-GGACCAAATCCAAACGAGAT-3′
ZmCYP97B	5′-CTGAGGAGAAGGACTTGACGG-3′	5′-TCCACTGGTCTGTCTGCGAT-3′
ZmCYP97C	5′-GTTGACATTGGATGTGATTGG-3′	5′-AACCAACCTTCCAGTATGGC-3′
Pacrtl	5′-ACCTCAACTGGCGAAACTGC-3′	5′-ACAGCGAGTGGAAAGAAAAC-3′
Gllycb	5′-GATTGGCGCGATTCACATCT-3′	5′-GCATGGCATAAAGAAAGGTGG-3′
Glbch	5′-CGGTGTTTGGAATGGCGTA-3′	5′-CGGAGTGATGAAGCGTGTGA-3′
ParacrtW	5′-GTGGCGCAAGATGATCGTCAAG-3′	5′-GCCAGAAGACCACGTACATCCA-3′
Zmactin	5′- CGATTGAGCATGGCATTGTCA-3′	5′- CCCACTAGCGTACAACGAA-3′

EXPERIMENTAL PROCEDURES

Transgenic plants

Four transgenic plant lines carrying various combinations of transgenes were selected for further analysis (Zhu *et al.*, 2008; Table 1). Endosperm samples were taken from immature seeds at 15, 20, 25, 30, 40, 50 and 60 days after pollination (DAP), frozen in liquid nitrogen and stored at −80°C.

Plants were sampled and analyzed in two consecutive seasons. No statistically significant differences were observed between the two sets of measurements for mRNA and metabolite analysis.

Total RNA isolation and quantitative real-time RT–PCR

Total RNA was isolated and RT–PCR was performed as decribed by Naqvi *et al.* (2009) using the primers listed in Table 3.

Modeling formalisms and model selection

Because no kinetic information was available for the enzymes participating in carotenoid biosynthesis, we invoked Ockham's razor, the principle stating that the explanatory hypothesis that is consistent with the observations and makes the fewest assumptions should be selected. Thus, we use the simplest possible formalism to represent the dynamics of the system (Alves *et al.*, 2008). This formalism is known as mass action, and has the following form:

$$\frac{dX_k}{dt} = \sum_{i=1}^{m} \mu_{i,k}\gamma_i \prod_{j=1}^{n} X_j^{fi,j}$$

where n is the number of dependent variables in the system, X_k is any of those dependent variables, m is the number of elementary processes occurring in the system, $\mu_{i,k}$ is the stoichiometric coefficient of X_k in process i, γ_i is the apparent rate constant for that process and $f_{i,j}$ is the apparent kinetic order of variable X_j in process i. If X_j is a substrate of the process, $f_{i,j}$ is given by its molecularity in the process; if not, $f_{i,j} = 0$.

Further details on model simplification, data interpolation, parameter fitting, aggregate enzyme activity profiles and statistical modelling of gene-enzyme correlations are provided in Methods S2.

ACKNOWLEDGEMENTS

This study was supported by the Ministerio de Ciencia e Innovación, Spain (BIO2007-61413, BIO2011-22525 and PM2010PKB-00746 CAROMAIZE) and a European Research Council Advanced Grant (BIOFORCE) to P.C. G.F. is the recipient of a PhD fellowship from the Ministerio de Ciencia e Innovación, Spain (BES-2008-003894). R.A. and A.S. are partially funded through Research Group 2009SGR809 from the Generalitat de Catalunya and through grants BFU2008-0196 to A.S. and BFU2010-17704 to R.A., both from the Ministerio de Ciencia e Innovación, Spain.

SUPPORTING INFORMATION

Additional Supporting Information may be found in the online version of this article.

Figure S1. Mathematical analysis of the models for the individual maize lines.

Methods S1. Carotenoid extraction, separation and identification.

Methods S2. Model simplification, data interpolation, parameter fitting, aggregate enzyme activity profiles and statistical modeling of gene–enzyme correlations.

Table S1. Correlating changes in aggregated enzyme activities to changes in gene expression for the genes involved in individual reactions for each maize line. The adjusted R^2 indicates the fraction of the flux variation in the reactions that consume LYC that could be explained by variations in the expression of the relevant genes.

Table S2. Correlating changes in aggregated enzyme activities to changes in gene expression for the genes involved in individual reactions for each maize line.

REFERENCES

Alves, R., Vilaprinyo, E., Hernández-Bermejo, B. and Sorribas, A. (2008) Mathematical formalisms based on approximated kinetic representations for modeling genetic and metabolic pathways. *Biotechnol. Genet. Eng. Rev.* **25**, 1–40.

Bai, C., Twyman, R.M., Farré, G., Sanahuja, G., Christou, P., Capell, T. and Zhu, C. (2011) A golden era-pro-vitamin A enhancement in diverse crops. *In Vitro Cell Dev. Biol.* **47**, 204–221.

Bartley, G.E. and Scolnik, P.A. (1994) Molecular biology of carotenoid biosynthesis in plants. *Annu. Rev. Plant Physiol. Plant Mol. Biol.* **45**, 287–301.

Blessin, C.W., Brecher, J.D., Dimler, R.J., Grogan, C.O. and Campbell, C.M. (1963) Carotenoids of corn and sorghum. V. Distribution of xanthophylls and carotenes in hand-dissected and dry milled fraction of yellow dent corn. *Cereal Chem.* **40**, 582–586.

Britton, G., Liaaen-Jenson, S. and Pfander, H. (2004) *Carotenoids Handbook*. Basel, Switzerland: Birkhauser Verlag.

Buckner, B., San-Miguel, P. and Bennetzen, J.L. (1996) The *y1* gene of maize codes for phytoene synthase. *Genetics*, **143**, 479–488.

Castillo, R., Fernandez, J.A. and Gomez-Gomez, L. (2005) Implications of carotenoid biosynthetic genes in apocarotenoid formation during the stigma development of *Crocus sativus* and its closer relatives. *Plant Physiol.* **139**, 674–689.

Chen, Y., Li, F. and Wurtzel, E.T. (2010) Isolation and characterization of the Z-ISO gene encoding a missing component of carotenoid biosynthesis in plants. *Plant Physiol.* **153**, 66–79.

D'Ambrosio, C., Giorio, G., Marino, I., Merendino, A., Petrozza, A., Salfi, L., Stigliani, A.L. and Cellini, F. (2004) Virtually complete conversion of lycopene into β–carotene in fruits of tomato plants transformed with the tomato lycopene β–cyclase (*tlcy–b*) cDNA. *Plant Sci.* **166**, 207–214.

Demmig-Adams, B. and Adams, W.W. (1996) The role of xanthophyll cycle carotenoids in the protection of photosynthesis. *Trends Plant Sci.* **1**, 21–26.

Farré, G., Sanahuja, G., Naqvi, S., Bai, C., Capell, T., Zhu, C. and Christou, P. (2009) Travel advice on the road to carotenoids in plants. *Plant Sci.* **179**, 28–48.

Farré, G., Bai, C., Twyman, R.M., Capell, T., Christou, P. and Zhu, C. (2011) Nutritious crops producing multiple carotenoids – a metabolic balancing act. *Trends Plant Sci.* **16**, 532–540.

Fraser, P.D., Truesdale, M.R., Bird, C.R., Schuch, W. and Bramley, P.M. (1994) Carotenoid biosynthesis during tomato fruit development. *Plant Physiol.* **105**, 405–413.

Fraser, P.D., Miura, Y. and Misawa, N. (1997) *In vitro* characterization of astaxanthin biosynthetic enzymes. *J. Biol. Chem.* **272**, 6128–6135.

Fraser, P.D., Shimada, H. and Misawa, N. (1998) Enzymic confirmation of reactions involved in routes to astaxanthin formation elucidated using a direct substrate *in vitro* assay. *Eur. J. Biochem.* **252**, 229–236.

Fujisawa, M., Takita, E., Harada, H., Sakurai, N., Suzuki, H., Ohyama, K., Shibata, D. and Misawa, N. (2009) Pathway engineering of *Brassica napus* seeds using multiple key enzyme genes involved in ketocarotenoid formation. *J. Exp. Bot.* **60**, 1319–1332.

Gallagher, C.E., Matthews, P.D., Li, F. and Wurtzel, E.T. (2004) Gene duplication in the carotenoid biosynthetic pathway preceded evolution of the grasses (Poaceae). *Plant Physiol.* **135**, 1776–1783.

Hirschberg, J. (2001) Carotenoid biosynthesis in flowering plants. *Curr. Opin. Plant Biol.* **4**, 210–218.

Jayaraj, J., Devlin, R. and Punja, Z. (2008) Metabolic engineering of novel ketocarotenoid production in carrot plants. *Transgenic Res.* **17**, 489–501.

Kim, M., Kim, S.C., Song, K.J., Kim, H.B., Kim, I.J., Song, E.Y. and Chun, S.J. (2010) Transformation of carotenoid biosynthetic genes using a micro-cross section method in kiwifruit. *Plant Cell Rep.* **29**, 1339–1349.

Li, F., Vallabhaneni, R., Yu, J., Rocheford, T. and Wurtzel, E.T. (2008) The maize phytoene synthase gene family: overlapping roles for carotenogenesis in endosperm, photomorphogenesis, and thermal stress tolerance. *Plant Physiol.* **147**, 1334–1346.

Li, F., Tzfadia, O. and Wurtzel, E.T. (2009) The *phytoene synthase* gene family in the grasses: subfunctionalization provides tissue-specific control of carotenogenesis. *Plant Signal. Behav.* **4**, 208–211.

Li, Q., Farré, G., Naqvi, S., Breitenbach, J., Sanahuja, G., Bai, C., Sandmann, G., Capell, T., Christou, P. and Zhu, C. (2010) Cloning and functional characterization of the maize carotenoid isomerase and β–carotene hydroxylase genes and their regulation during endosperm maturation. *Transgenic Res.* **19**, 1053–1068.

Lima, V.L., Melo, E.A., Maciel, M.I.S., Prazeres, F.G., Musser, R.S. and Lima, D.E. (2005) Total phenolic and carotenoid contents in acerola genotypes harvested at three ripening stages. *Food Chem.* **90**, 565–568.

Liu, Y., Gur, A., Ronen, G., Causse, M., Damidaux, R., Buret, M., Hirschberg, J. and Zamir, D. (2003) There is more to tomato fruit colour than candidate carotenoid genes. *Plant Biotechnol. J.* **1**, 195–207.

Maass, D., Arango, J., Wust, F., Beyer, P. and Welsch, R. (2009) Carotenoid crystal formation in Arabidopsis and carrot roots caused by increased phytoene synthase protein levels. *PLoS One*, **4**, e6373.

Maluf, M.P., Saab, I.N., Wurtzel, E.T. and Sachs, M.M. (1997) The *viviparous12* maize mutant is deficient in abscisic acid, carotenoids, and chlorophyll synthesis. *J. Exp. Bot.* **48**, 1259–1268.

Misawa, N., Truesdale, M.R., Sandmann, G., Fraser, P.D., Bird, C., Schuch, W. and Brambley, P.M. (1994) Expression of a tomato cDNA coding for phytoene synthase in *Escherichia coli*, phytoene formation *in vivo* and *in vitro*, and functional analysis of the various truncated gene products. *J. Biochem.* **116**, 980–985.

Moran, N.A. and Jarvik, T. (2010) Lateral transfer of genes from fungi underlies carotenoid production in aphids. *Science*, **30**, 624–627.

Naqvi, S., Zhu, C., Farre, G. *et al.* (2009) Transgenic multivitamin corn through biofortification of endosperm with three vitamins representing three distinct metabolic pathways. *Proc. Natl Acad. Sci. USA*, **106**, 7762–7767.

Naqvi, S., Zhu, C., Farré, G., Sandmann, G., Capell, T. and Christou, P. (2011) Synergistic metabolism in hybrid corn indicates bottlenecks in the carotneoid pathway and leads to the accumulation of extraordinary levels of the nutritionally impotant carotenoid zeaxanthin. *Plant Biotechnol. J.* **9**, 384–393.

Pogson, B., McDonald, K., Truong, M., Britton, G. and DellaPenna, D. (1996) Arabidopsis carotenoid mutants demonstrate lutein is not essential for photosynthesis in higher plants. *Plant Cell*, **8**, 1627–1639.

Pozniak, C.J., Knox, R.E., Clarke, F.R. and Clarke, J.M. (2007) Identification of QTL and association of a phytoene synthase gene with endosperm colour in durum wheat. *Theor. Appl. Genet.* **114**, 525–537.

Quinlan, R.F., Jaradat, T.T. and Wurtzel, E.T. (2007) *Escherichia coli* as a platform for functional expresión of plant P450 carotene hydroxylases. *Arch. Biochem. Biophys.* **458**, 146–157.

Ravanello, M.P., Ke, D., Alvarez, J., Huang, B. and Shewmaker, C.K. (2003) Coordinate expression of multiple bacterial carotenoid genes in canola leading to altered carotenoid production. *Metab. Eng.* **5**, 255–263.

Rissler, H. and Pogson, B.J. (2001) Antisense inhibition of the β–carotene hydroxylase and nonphotochemical quenching in Arabidopsis. *Photosynth. Res.* **67**, 127–137.

Romer, S., Lubeck, J., Kauder, F., Steiger, S., Adomat, C. and Sandmann, G. (2002) Genetic engineering of a zeaxanthin-rich potato by antisense inactivation and co-suppression of carotenoid epoxidation. *Metab. Eng.* **4**, 263–272.

Rosati, C., Aquilani, R., Dharmapuri, S., Pallara, P., Marusic, C., Tavazza, R., Bouvier, F., Camara, B. and Giuliano, G. (2000) Metabolic engineering of β–carotene and lycopene content in tomato fruit. *Plant J.* **24**, 413–419.

Steenbock, H. and Coward, K.H. (1927) Fat-soluble vitamins. XXVII. The quantitative determination of vitamin A. *J. Biol. Chem.* **72**, 765–779.

Taylor, M. and Ramsay, G. (2005) Carotenoid biosynthesis in plant storage organs: recent advances and prospects for improving plant food quality. *Physiol. Plant.* **124**, 143–151.

Van Eck, J., Conlin, B., Garvin, D.F., Mason, H., Navarre, D.A. and Brown, C.R. (2007) Enhancing β–carotene content in potato by RNAi-mediated silencing of the β–carotene hydroxylase gene. *Am. J. Potato Res.* **84**, 331–342.

Wong, J.C., Lambert, R.J., Wurtzel, E.T. and Rocheford, T.R. (2004) QTL and candidate genes phytoene synthase and zetacarotene desaturase associated with the accumulation of carotenoids in maize. *Theor. Appl. Genet.* **108**, 349–359.

Ye, X., Al-Babili, S., Kloti, A., Zhang, J., Lucca, P., Beyer, P. and Potrykus, I. (2000) Engineering the provitamin A (β–carotene) biosynthetic pathway into (carotenoid-free) rice endosperm. *Science*, **287**, 303–305.

Zhu, C., Naqvi, S., Breitenbach, J., Sandmann, G., Christou, P. and Capell, T. (2008) Combinatorial genetic transformation generates a library of metabolic phenotypes for the carotenoid pathway in maize. *Proc. Natl Acad. Sci. USA*, **105**, 18232–18237.

Zhu, C., Naqvi, S., Capell, T. and Christou, P. (2009) Metabolic engineering of ketocarotenoid biosynthesis in higher plants. *Arch. Biochem. Biophys.* **483**, 182–190.

Zhu, C., Bai, C., Sanahuja, G., Yuan, D., Farré, G., Naqvi, S., Shi, L., Capell, T. and Christou, P. (2010) The regulation of carotenoids pigmentation in flowers. *Arch. Biochem. Biophys.* **504**, 132–141.

